Friction **12**(5): 954–967 (2024)
https://doi.org/10.1007/s40544-023-0813-z
ISSN 2223-7690
CN 10-1237/TH
RESEARCH ARTICLE

Stable graphene oxide-based lyotropic liquid crystals for interfacial lubrication

Yumei GUO[1,2], **Hanglin LI**[1], **Jiusheng LI**[1], **Xiangqiong ZENG**[1*]

[1] *Laboratory for Advanced Lubricating Materials, Shanghai Advanced Research Institute, Chinese Academy of Sciences, Shanghai 201210, China*

[2] *University of Chinese Academy of Sciences, Beijing 100049, China*

Received: 17 April 2023 / Revised: 05 July 2023 / Accepted: 02 August 2023

Abstract: Lyotropic liquid crystals have lubricating properties due to their ordered assembly and fluidity, whose mesogens are often characterized by amphiphilic properties. Despite the attention that graphene oxide (GO) has been studied as a novel amphiphilic lyotropic mesogen this decade, and GO applied as a lubrication additive has been demonstrated in both oil and water-based systems, little research reveals the interfacial lubrication of GO liquid crystals yet. This work reports that GO aqueous dispersion can form lyotropic liquid crystals above a specific critical concentration of 5.00 mg/mL, providing a form of stable water-based lubricant, which can keep stable for several months and can reduce friction by 37.3% and wear by 25.24%. The liquid crystal phase was verified by polarizing microscope and synchrotron radiation small-angle X-ray scattering, and its rheological properties and viscoelasticity were studied by interfacial rheometer. The formation of lyotropic liquid crystals can enhance the stability of GO aqueous dispersions at high density, simultaneously ensuring friction decrease and anti-wear effect. It is attributed to the stable nematic network by the ordered GO sheets. The ordered assembly structure bears vertical shear force, therefore, reducing the wear. It is also assumed that the wide lateral size of graphene oxide promotes the nematic phase thus smoothes the graphene oxide film composed spontaneously under the coincidence of lamellar liquid crystal and 2D layered material. Through this work, the interlayer lubrication of GO was optimized, and the problem of GO dispersion sedimentation was solved by self-assembly. The range of interfacial lubrication of GO aqueous dispersion has been expanded and the synergistic effect is conducive to the environmentally friendly lubricants.

Keywords: lyotropic liquid crystal; graphene oxide; aqueous lubrication; tribological behavior

1 Introduction

The special lubricating properties of lyotropic liquid crystals (LLCs) are often used in natural like biological lubricating systems, and nematics and cholesterics perform the talented practical application [1]. Gradually, the range of lyotropic liquid crystal phases is extended to amphiphilic compounds and surfactants which can self-organize into highly ordered yet fluid, phase-segregated assemblies in the presence of a polar liquid such as water [2]. Onsager's theory reveals the formation of nematic liquid crystals from the pure entropy drive mechanism [3, 4], showing the liquid crystal phase dependence on the critical concentration, size, and shape. Above the critical concentration to form the LLC phase, it is nematically stable. At higher concentrations, the anisotropic particles have more large repelling volumes that induce entropy loss. The LC phase is the truly thermodynamically stable state of matter combining the characteristics of both a solid (anisotropy/orientational order) and a liquid (fluid property/collective mobility), exhibiting interesting

* Corresponding author: Xiangqiong ZENG, E-mail: zengxq@sari.ac.cn

rheological properties, exciting optical, mechanical, viscoelastic, and dielectric properties. A wide range of nanomaterials, including metallic, semiconducting, biological, and pharmaceutical origin, have been identified as LCs with nematic, smectic, lamellar, and hexagonal mesophases [5]. This phenomenon has been observed in graphene-based colloidal systems.

Graphene oxide (GO) can be treated as amphiphilic material with an edge-to-center distribution of hydrophilic and hydrophobic domains at interfaces [6–8], igniting new self-assemble strategies and dispersing agent development [9]. After Behabtu et al. reported the exfoliated monolayer graphene in chlorosulfonic acid and the spontaneous formation of liquid crystal phase at high concentrations (20–30 mg·mL^{-1}) in 2010 [10], subsequently Kim et al. verified the liquid crystallinity of graphene oxide water dispersant for the first time [11]. A special issue on the subject of "Graphene Oxide Liquid Crystals" has been compiled from basic fundamental properties of GOLCs to their versatile applications [12]. Xu and Gao found that as the concentration increases, the optical texture becomes more compact, and with the Zeta potential of about –64 mV for GO dispersions, with the absolute value decreased with increasing salt, proving that electrostatic repulsion between negatively charged GOs is the dominant interaction in the GO liquid crystal system [13]. Graphene oxide liquid crystal (GOLC) with different types of liquid crystal phases, such as nematic, lamellar, and chiral phases, is controlled by several key parameters governing the ultimate stability of GOLC behavior, including pH and ionic strength of aqueous dispersions [14]. The confinement volume and geometry relative to the particle size are critical for the observation of the LLC phase, which determines the critical concentration [15]. Aboutalebi et al. first proposed a method to prepare a single-layer GO sheet mesogen with a large area (10,000 μm^2), which reduced the critical concentration of liquid crystal formation to 0.1 wt% [16]. The oxygen functional groups, which cause secondary interactions between GOs, decrease the critical concentration for the phase transitions from isotropic to biphasic to nematic phases, and the strong hydrogen bonding networks between GO sheets govern the stabilization of the GO aqueous dispersion for a long period [17].

Graphene acts as a new emerging lubricant and exhibits the tribological performance from nano-scale to micro-scale even up to macro-scale, including the oxides, modifiers, and other derivatives [18–20]. The effect of pH on their microstructure and tribological performance was systematically assessed that acidic GO suspension (pH 3.10) effectively reduced the coefficient of friction (COF) by 44.4% and wear radius by 17.1% [21]. Liu et al. reported the progress of 2D materials which have a high specific surface area, in-plane strength, weak layer-layer interaction, and surface chemical stability, resulting in remarkably low friction and wear-resisting properties, and presented the challenge of the limit of the agglomeration of grapheme [22]. The modification of long alkyl chains and active sulfur elements into the GO sheets will improve the dispersion stability and tribological properties in rapeseed oil [23]. Aminoborate-functionalized reduced graphene oxide for aqueous lubricants exhibited 20 days of dispersion stability and improved the thermal conductivity of water [24]. Aminated silica modified graphene oxide improves the aqueous short-term stability and strengthens the wear-resistance [25]. Despite, whether chemical modification or functionalization, ultra-low concentration additives still face the problem of poor dispersion stability and aggregation effect in lubricating systems.

Advances in nanoscience promote the study of liquid crystals to orient anisotropic colloids to broaden the application of graphene oxide materials [26], mainly focusing on how to rationally control the formation and processability of GO liquid crystal dispersions to develop bottom-up device fabrication processes [27, 28] or hydrogels with mechanical strength to nanofluidic ionic cables [29]. However, the high stability brought by the ordered self-assembled liquid crystal phase of GO has insufficient attention and even less research on lubrication, while GO attracts high attention as lubrication additives [19]. The dispersion stability, structural characteristics, and dosage, as well as contact geometry of graphene-based dispersions, play important roles in affecting the tribological properties [30]. How to solve the problem of agglomeration and precipitation is the key to the lubricant additive.

Although there were studies on the tribological behavior of GO and on the liquid crystal behavior of GO respectively, there was little research on revealing the frictional behavior of GO-based liquid crystal, which may not only enhance the stability of graphene oxide aqueous dispersion via lyotropic liquid crystal structure without chemical reaction but also exhibit promising tribological properties due to the combined effect of GO and liquid crystal. Since it is promising to exploit amphiphilic self-assembly of surfactants to form nematic liquid crystals as environmentally friendly lubricants, the construction of a lubricating system of graphene oxide based lyotropic liquid crystals is expected to exert a synergistic effect and is also of great value for practical applications.

2 Experimental details

2.1 Preparation

2.1.1 Materials

The mass-produced GO (SE2430, Changzhou Sixth Element Material Technology Co. Ltd.) was named as GO directly in the following section. Graphite (500 mesh, J&K Scientific Ltd., 99%), H_2SO_4 (Sinopharm Chemical Reagent, 98%), $KMnO_4$ (Sinopharm Chemical Reagent., 98%), and H_2O_2 (Sinopharm Chemical Reagent., 30 wt%) were used to prepare graphene oxide with a higher degree of oxidation in the laboratory via improved Hummers method [31], which was named as GO-lab next.

2.1.2 Methods

GO liquid crystal (GOLC) was prepared in an ultrasonic ice bath (Scientz, SB-5200DTD, Ningbo, China) with an input power of 250 W and a frequency of 40 kHz. GO dispersion of a certain concentration（0.15 mg/mL, 0.20 mg/mL, 0.50 mg/mL, 1.00 mg/mL, 2.5 mg/mL, 5.00 mg/mL, and 10 mg/mL) was ultrasonically dispersed for 2 h, with occasional stirring at least every 30 min until no precipitation. Ultrasound will heat water, and ice needs to be added to control the temperature below room temperature. If the system does not have obvious precipitation after standing for 3 days, it indicates that the system tends to be stable, and if the system still has no obvious precipitation after standing for 7 days, it indicates that the liquid crystal system is formed. For systems below the critical concentration of liquid crystals, ultrasonic dispersion can only keep them stable for a short time, usually no more than 2 days.

2.2 Characterization

GO-lab and GO were identified by X-ray diffraction (XRD, Rigaku Ultima IV, Japan), attenuated total reflectance (ATR, Paragon 1000, Perkin Elmer, USA) of FTIR infrared spectroscopy, Raman (Horiba HR Evolution, France), and UV–Vis spectrophotometer (UV-4802S, UNICO, USA). The stability of GO dispersion and GOLC was monitored via the change of UV absorption during a month. The microsurface topography was collected using scanning electron microscopy (SEM, Zeiss Gemini 300, Germany) and atomic force microscope (AFM, Bruker Dimension Icon Germany). The liquid crystal texture was displayed under optical polarizing microscopy (POM, XP-330C, Caikang, China) and small-angle X-ray scattering (SAXS) at Beamline BL19U2 of Shanghai Synchrotron Radiation Facility. The surface tension of dispersion was measured at room temperature with an interface rheometer (DSA30R, KRUSS, Germany) based on the pendant drop technique. For interfacial dilatational rheology, we apply the video-enhanced pendant drop method with an oscillation drop module (ODM) to obtain E (complex viscoelastic modulus), E' (storage modulus), and E'' (loss modulus) derived. The characteristic distribution of graphene composition on wear surfaces was recorded on a DXRTM Raman spectrometer (Thermo Fisher Scientific, USA) with mapping images. The morphological and microstructural surfaces of the wear scars were complemented by SEM equipped with energy-dispersive spectroscopy (EDS, Oxford Xplore, UK).

2.3 Tribological measurements

The interfacial lubricating characteristics of the developed GO based lyotropic liquid crystal was studied by using the UMT-Tribolab (Bruker, USA) to do the tribological testing with rotation mode and the frictional pairs composed of the upper ball (d=5 mm, bearing steel) and stationary plate (d=60 mm, 304 stainless steel sheet). All tests were

conducted under a load of 3 N and with a friction speed of 200 mm/s to a distance of 180 m, resulting in 1.014 GPa for Hertzian contact pressure. A three-dimensional optical surface profiler (Countour GT-K, Bruker, USA) was used to measure the stereoscopic topography and wear volume of the worn surface after the friction test, working jointly with Raman scan mapping and SEM-EDS mapping to analyze the composition of the interfacial lubrication film. The wear rates were calculated from the steady state region of the real-time wear plots excluding the running-in phase [32].

3 Results

3.1 Characterization of GO-lab and GO

The results of XRD (Fig. 1(a)) show that both GOs have one strong and one weak peak [33]. The positions of the weak peaks are similar, all-around 42°, but shift to the left compared with the weak peaks of graphite, indicating that there is a small amount of residual graphite. The mass-produced GO sample has a GO characteristic peak at 11.8° (d=0.749 nm), and the GO-lab is at 10.3° (d=0.858 nm). Combined with the Bragg equation, it shows that the interlayer distance of the GO-lab is larger and the degree of oxidation is higher. However, the peak intensity of mass-produced GO is larger, and the crystallinity may be higher. The FTIR results (Fig. 1(b)) show that the positions and intensities of the main oxygen-containing functional groups are roughly in agreement with the general FTIR results, but are slightly different, with a small broad peak around 2,800 cm^{-1}, mainly due to alkyl chain stretching vibrations. Both D peaks (about 1,340 cm^{-1}) and G peaks (about 1,580 cm^{-1}) appear in the Raman spectra (Fig. 1(c)). The G peak shows the sp^2 hybridized carbon skeleton structure, and the D peak represents the defect peak of the carbon skeleton due to oxidation. The integrated area ratio (I_D/I_G) of the D peak and the G peak obtained after the Raman spectrum fitted and processed by Origin software can roughly estimate the content ratio of sp^3 hybridized carbon atoms and sp^2 hybridized carbon atoms, thereby distinguishing graphite ordered and disordered crystal structures. It is found by calculation that the I_D/I_G (=2.45) of the GO-lab is significantly higher than that of the mass-produced GO (=1.89), indicating that the GO-lab had a higher degree of oxidation, which resulted in more defects. UV absorption spectra (Fig. 1(d)) show that both GO samples have an absorption peak near 230 nm, attributed to the π→π* transition of the C=O bond, and a shoulder at 300 nm, attributed to the n→π* transition of the C=O bond π* transition. Raman and UV-Vis results are also consistent with the literature [34]. The morphologies of the two GOs are shown in Figs. 1(e)–1(h), the GO-lab has more wrinkles

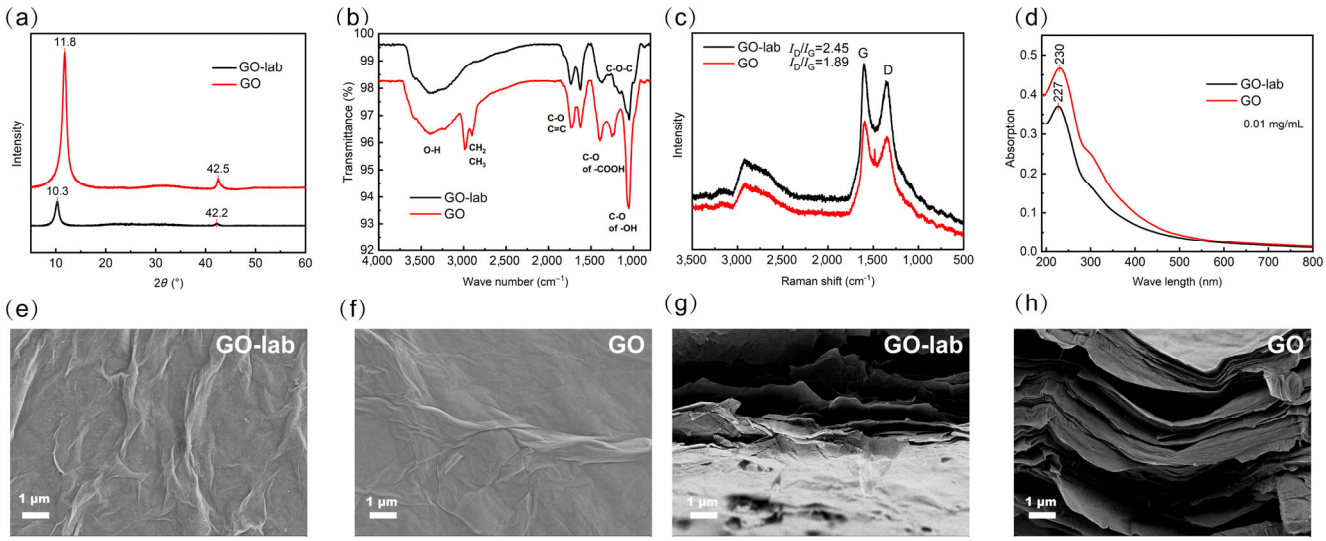

Fig. 1 Characterization of GO-lab and GO. (a) XRD, (b) FTIR, (c) Raman, (d) UV-Vis, (e, f) SEM of surface, (g, h) SEM of side section.

(Fig. 1(e)) from the surface, and the interlayer spacing from the cross-section of the film is larger (Fig. 1(g)), for the reason that more oxygen functional groups resulted in rough defects leading to folds and space hindrance during the layer-by-layer secondary assembly. Mass-produced GO can obtain a highly ordered layer-assembled membrane structure (Fig. 1(h)) after solvent evaporation without using precision instruments or vacuum filtration technology, which corresponds to the self-assembled membrane obtained by GO liquid crystal transitions with an aspect ratio of over 30,000 prepared by Aboutalebi et al. [16]. The Hummers method (concentrated sulfuric acid) dominates as the mainstream strategy to synthesize GO [35].

The AFM results of the two GOs are shown in Fig. 2, for displaying the degree of exfoliation of graphite oxide in the aqueous dispersion and their lateral size and thickness. The GO-lab has a smaller lateral size and a sheet thickness of about 1.2 nm (Fig. 2(c)), while the mass-produced GO has a micron-scale lateral size with a sheet thickness of about 1.5 nm (Fig. 2(f)). It can be inferred that GO-lab has a higher oxidation degree accompanied by relatively smaller sheet thickness, resulting in better hydrophilic performance [36, 37]. More hydrogen bonds between epoxides and hydroxyl groups indicated high binding energy and thus increased shear strength [35, 36]. The different properties of the two GOs in terms of oxidation degree and promotion of liquid crystal phase formation may lead to a competitive relationship rather than a synergistic relationship in friction reduction and anti-wear performance.

3.2 The construction and characteristics of GO dispersion and GOLC

3.2.1 *The influence of GO concentration on the formation of liquid crystal*

The oxygen functional groups on the surface of the graphene layer make GO amphiphilic, which facilitates the formation of graphene oxide liquid crystals. Liquid crystals usually have ordered microstructures that are formed by the self-assembly of their constituent units driven by competition for filling and orientation entropy, GO can form LCs and its LC behavior depends on the size and concentration of GO sheets and factors such as the viscosity of the solvent.

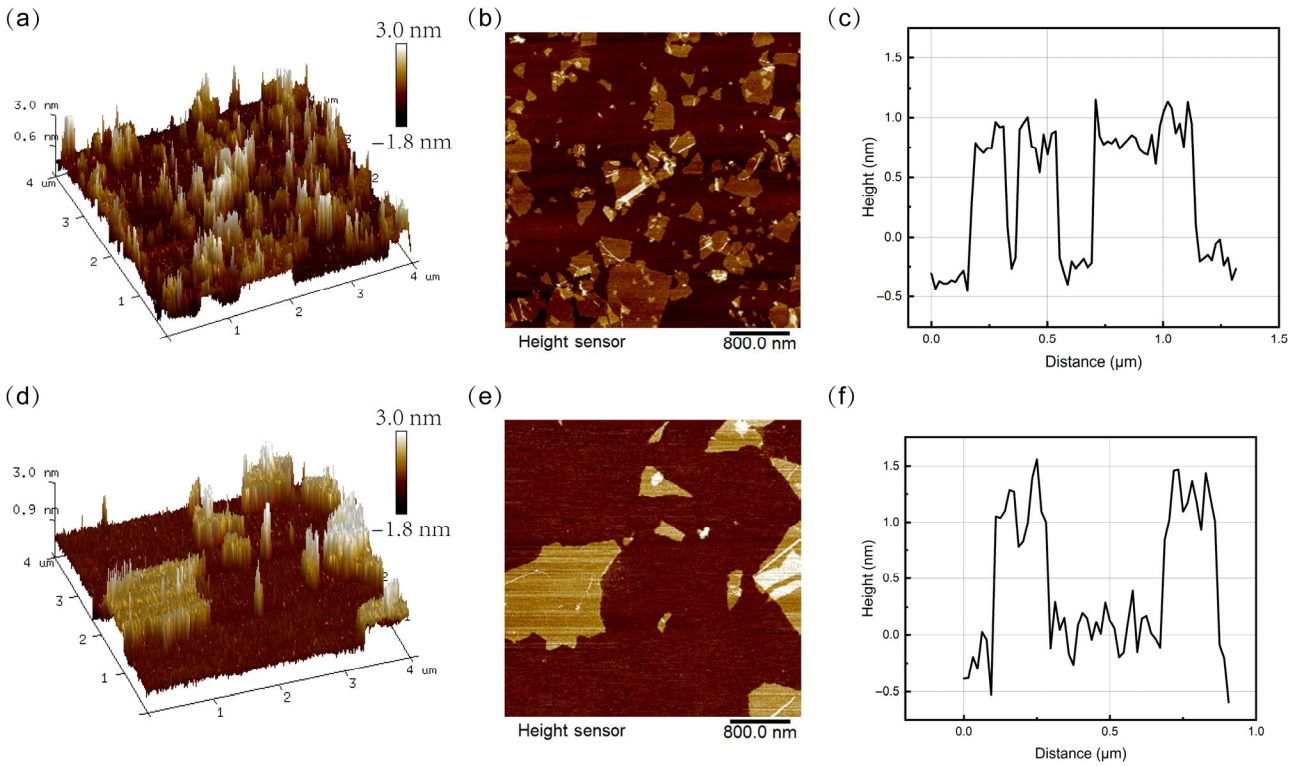

Fig. 2 AFM images: (a–c) GO-lab; (d–f) GO.

In the case of using ordinary-sized GO sheets (average size < 10 μm), the formation of highly oriented liquid crystals requires high concentrations (10 mg/mL), while alkalis such as KOH can induce the formation of highly ordered textures in GO liquid crystals [37]. According to the Onsager model and liquid crystal phase diagram corresponding with aspect ratio and concentration, larger-sized GO can form nematic liquid crystals at lower concentrations [13].

The phase diagram of the two kinds of GO is observed in Fig. 3. By adjusting the crossed polarizer to 90°, periodic bright and dark states can be observed, while the bright regions of GO are scattered and show anisotropic phase, especially on larger sheets. Low concentration (5.00 mg/mL, 0.5 wt%) GO can only form scattered isotropic-nematic phase under POM (Figs. 3(c) and 3(d)), while high concentration (10 mg/mL) GO can form large nematic liquid crystals with certain regularity (Figs. 3(a) and 3(b)) [38]. In the biphasic GO dispersion where both isotropic and liquid crystalline phases are equilibrated (Fig. 3(a)), more densities of GO texture are spontaneously concentrated within the liquid crystalline phase [39]. A larger aspect ratio allowed GO dispersion tendency to the GOLC network. The transition from pseudo-isotropic to biphasic to nematic state can be observed from Fig. 3(c) to Fig. 3(a) to Fig. 3(b), ultimately uniform birefringence indicates a homogeneous alignment of GOLC. Large-scale mass-produced GO may be more suitable for further investigation of liquid crystal phases. Therefore despite high oxidation leading to better aqueous solubility, aspect ratio matters greatly on ordered self-assembly. The thermal stability of GOLC has also been confirmed. Below the reduction temperature of GO to rGO (165 °C), in the temperature range of 25–100 °C, the volatilization of water guides the liquid crystal phase to align in a more ordered direction [40]. GO has spectacular advantages in the preparation of self-assembly and functional membrane, which is also consistent with the periodic arrangement of liquid crystals.

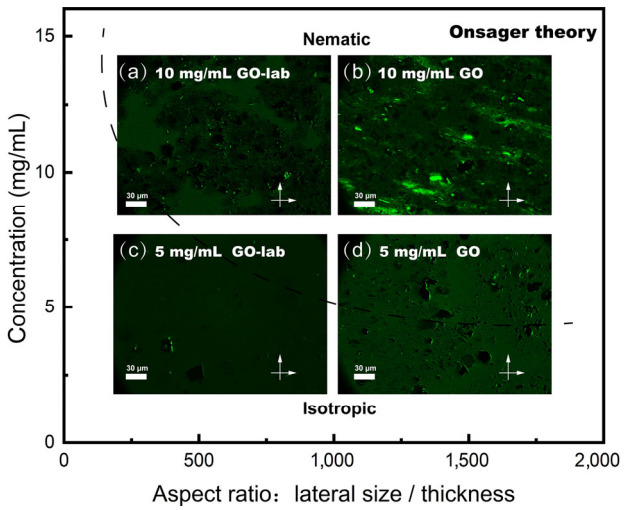

Fig. 3 POM of GO liquid crystals: (a) GO-lab 10.00 mg/mL, (b) GO 10.00 mg/mL, (c) GO-lab 5.00 mg/mL, (d) GO 5.00 mg/mL.

The structure of GOLC demands further confirmation to reveal the critical concentration via SAXS. Figure 4 clearly shows the synchrotron radiation SAXS results of different phases of GO dispersions at different concentrations. In the range of 0 to 10.00 mg/mL, the signal images in the 2D scatter pattern gradually transits from a uniform ring (under 2.50 mg/mL) to an ellipse (under 5.00 mg/mL), until an oblate deformation shaped like a nebula at 10.00 mg/mL [13]. It demonstrates that the critical concentration of GOLC locates near 5.00 mg/mL. SAXS *in situ* rheology ever reveals that the flow-induced alignment of GO is more subtle, consequently flow velocity leads to different fractions of materials aligning along different directions and the spacing between the flakes decreases in response to viscous forces [38].

3.2.2 *The interfacial rheological characteristics and stability of GO dispersion and GOLC*

Pseudoplastic type non-Newtonian behavior (shear-thinning) could happen in GO nanofluid [39], thus

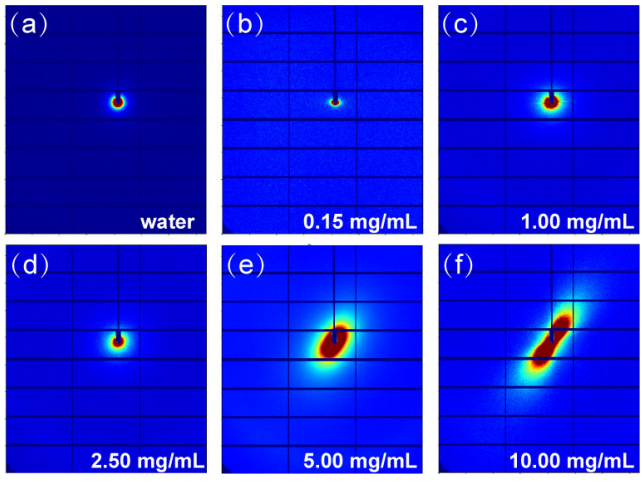

Fig. 4 SAXS 2D pattern of GO dispersion with different concentrations: (a) 0, (b) 0.15, (c) 1.00, (d) 2.50, (e) 5.00, (f) 10.00 mg/mL.

GO dispersions act as thixotropic fluids since GO aggregates are reversibly formed once the flow is arrested [40]. Figure 5 shows the evolution of viscosity versus the shear rate of GO dispersion at different concentrations. The regular pattern of the flow separates from low and high shear regions. Since water belongs to a typical Newtonian fluid, as the shear rate increases, the steady flow of which in the high shear region means reference value. The matrix fluid dominates at a relatively low concentration, while the interaction between the base fluid and the nanoparticles plays an important role in the rheological properties of the nanofluid at a higher concentration [41]. At the high shear region, the rheological behavior changes from nearly still to shear-thinning as the concentration increases. It indicated that the formation of the GO liquid crystal phase made an effect, above 5.00 mg/mL [42, 43]. GO of 10.00 mg/mL exhibits a higher viscosity and GO at the critical concentration with different oxidation degrees shows consistent viscosity and rheological behavior. GO microstructure has been reported to strongly shear-dependent and GO suspensions with a shear threshold for optimal alignment, allowed achieving the tensile strength and Young's modulus improvement of the graphene fibers prepared subsequently without any chemical modification [44].

In addition, an amphiphile GO sheet can be seemed as a surfactant by its ability to absorb and decrease the surface or interfacial tension [7]. Figure 6 shows the surface tension of GO dispersions and GOLC

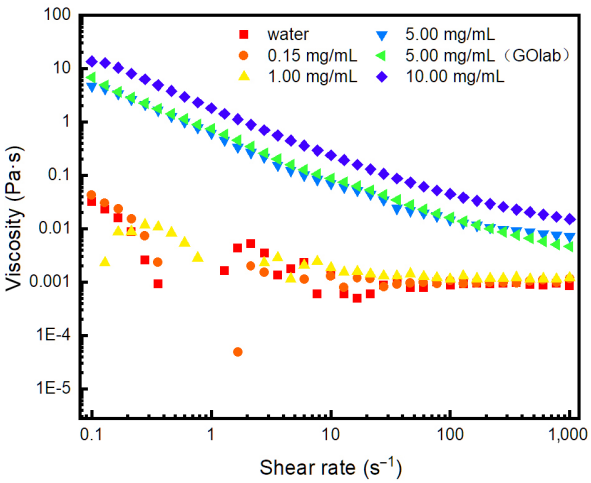

Fig. 5 Evolution of shear viscosity with the shear rate at different concentrations.

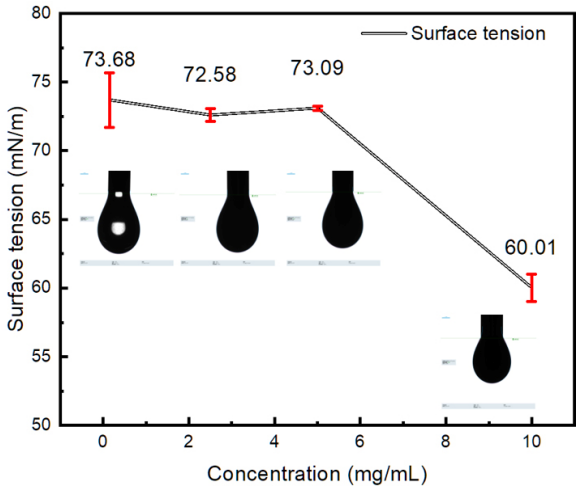

Fig. 6 Surface tension of GO dispersion.

with different concentrations. Based on the Young Laplace equation, despite there being no significant surface activity for GO below the critical concentration, GO of 10 mg/mL reduces the surface tension of water from 73.68 mN/m to 60.01 mN/m. The decreasing surface tension versus concentration manifests the activity and stability of GO sheet at air/liquid interfaces and block moisture evaporation, which is conducive to the use of its surface activity for 2D self-assembly [6].

GO suspensions consisting of platelets of high aspect ratios form exceptional viscoelastic gel [45] and mechanical membrane [46–48]. GO dispersions exhibit unique viscoelastic behavior, varying considerably with concentration. The dilational rheology reveals the interfacial resistance to changes in the interface area and the variation of system energy as a function of interfacial area [49, 50]. Since the loss modulus (E'') due to internal heat dissipation maintains small values, the complex viscoelastic modulus (E) is dominated by the storage modulus E' ($E = E' + iE''$) [51, 52]. Figure 7 shows the corresponding modulus variation with GO concentration as the rule previously reported. Above critical concentration, as the nematic LC phase form, a further increase in the volume fraction results in a simultaneous increase in both modulus, with the storage modulus increasing much faster than the loss modulus [53]. By increasing the GO concentration from 5 to 10 mg/mL, E increases by more than 30 mN/m. The observed increase in swelling elastic modulus with more GO indicates that the nanosheets are adsorbed at the interface [54].

By introducing damping materials, whose damping factor or loss factor ($\tan\psi = E''/E'$) [55] was described, their deformation dissipates the vibrational energy of the friction system and reduces severe wear at the contact interface [56]. In Fig. 7(b), all damping factors <1, which indicates that the storage modulus takes precedence over the loss modulus. Although the internal friction and the viscous part in the system increase, the elastic part still dominates the viscous part, resulting in an overall flexible system with an increased viscous part [57].

The stability of GO aqueous solution with an insufficient degree of oxidation has great limitations. Owing to the too dark and opaque color to show the stable superiority of GOLC in photos, the content of GO in the upper layer was verified by UV spectrophotometry [24]. Figure 8 shows the UV absorption of GO dispersion and GOLC over time. For all GO dispersion, at each test point, the upper layer was taken out and diluted to 0.01 mg/mL, and the absorbance was collected at 228 nm. It is found

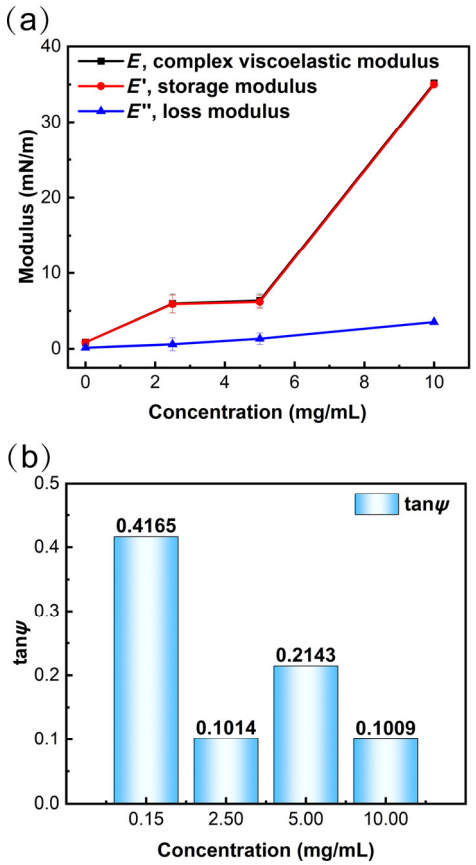

Fig. 7 Corresponding modulus variation with GO concentration: (a) viscoelasticity modulus, (b) tanΨ.

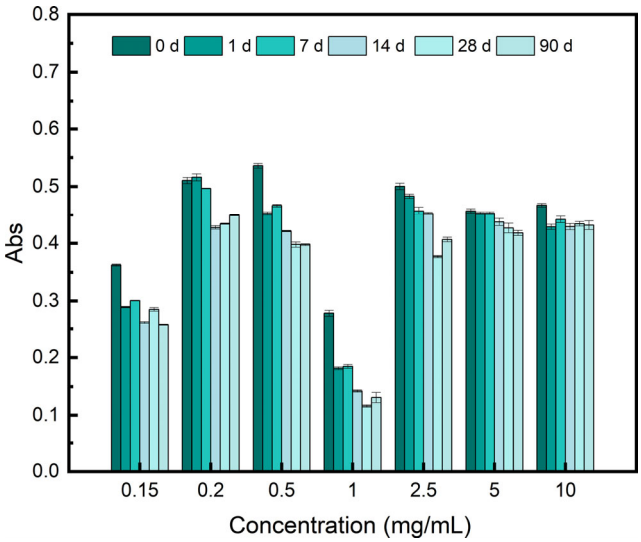

Fig. 8 Stability of GO dispersion and GOLC using UV-absorption during three months.

that the absorbance of the upper layer of GO in the low concentration sample decreases with time. According to Lambert Beer's law, the GO concentration becomes less than the initial value corresponding to the decreasing absorbance. Yet the absorbance of GOLC remained stable for several months, indicating that the bulk phase of GOLC was uniformly dispersed indeed, and the formation of LC can significantly improve the stability of GO dispersion.

3.2.3 *The interfacial lubricating characteristics of GO liquid crystal*

The water dispersibility of GO introduced with oxygen-containing functional groups is greatly enhanced, and it has also been studied as a water-based lubricant. The friction coefficient and wear rates of GO dispersions with different concentrations are shown in Fig. 9 to reveal the interfacial lubricating characteristics of GO dispersions. It is clear that the addition of GO can significantly reduce the COF of water. Additive concentrations can be optimized as low as 0.15 mg/mL (friction decreased by 49.1% and wear decreased by 41.7% compared to that of water), where the material with higher oxidation exfoliated to smaller sheets has better hydrophilicity and dispersibility in the low concentration range [31]. Increasing from 0.15 mg/mL to 0.50 mg/mL, both COF and wear increase with concentration. Moreover, the optimized concentration (1.00 mg/mL and 5 mg/mL) is surprisingly consistent

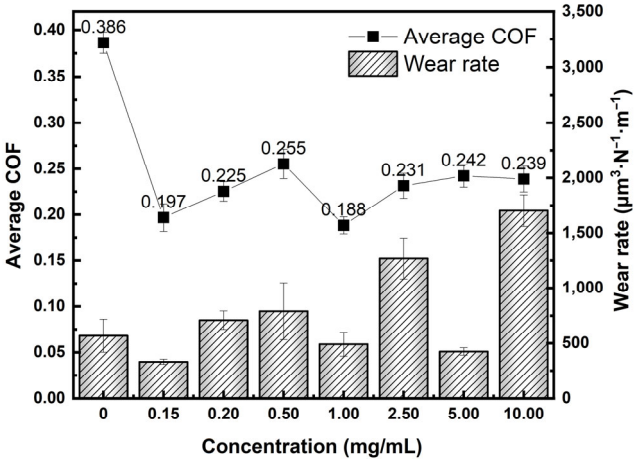

Fig. 9 Average coefficient of friction and wear rate of different concentrations of GO dispersed in water.

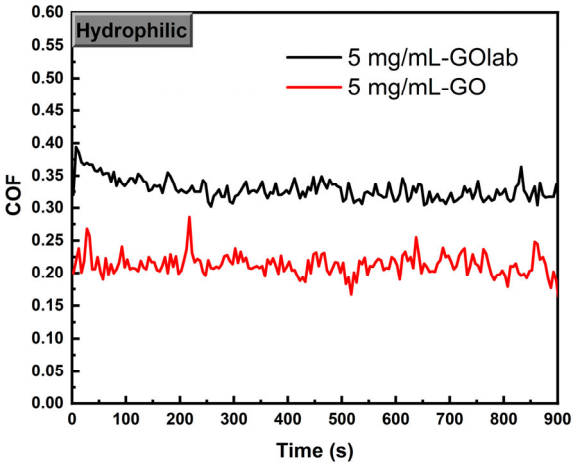

Fig. 10 Friction curves of GO with two different lateral dimensions and hydrophilicity.

with the results reported by Singh et al. [58]. When the addition amount is 1.00 mg/mL as a turning point of low and high concentration, and the COF is as low as 0.188, which is 51.3% lower than that of pure water. Yet 1.00 mg/mL GO has the worst stability (Fig. 7). Above 1.00 mg/mL, the COF increases and then keeps almost stable after the formation of the liquid crystal phase. It seems that high concentrations of GO (2.50 mg/mL) without LC are not favored, for wear rates are even more serious than GOLC with 5.00 mg/mL which greatly reduces friction by 37.3% and wear by 25.2%. However, when the concentration is 10.00 mg/mL, the COF stays almost the same as that at 2.50 mg/mL and 5.00 mg/mL, but the wear increases a lot. It is speculated that GOLC network saves steady state from aggregation during the sliding process exceeds liquid crystal lubrication. Considering GO can be induced by shear to form a stable, periodic, and macroscopic alignment in a wide shear range [59]. It is referred that there is a macroscopic upper limit to GOLC lubrication at the friction interface, with the arrangement of larger lamellae arousing more critical wear. In the liquid crystal phase range with more nanosheets, without the agglomeration of GO in a disordered state caused by rapid shearing [60], improved mechanical ability can be observed. Therefore, the larger size of GO can restore the liquid crystal phase faster to maintain the stability of the lubricating system, leading to a lower coefficient of friction (Fig. 10).

3.3 The interfacial lubricating mechanism of GO liquid crystal

Based on previous studies on the tribological properties of graphene additives, the lubrication mechanism can be summarized into the following four aspects: tribo-film formation, microstructural transformation, interlayer slip, and synergistic effects [20]. Characterization of wear scar surfaces was carried out via 2D Raman and SEM-EDS. The G/D peaks of the spectra in Fig. 11 can be attributed to the Raman scattering of GO. From the 2D Raman scan mapping of the scars, it can be referred that due to the high surface activity caused by the nano-size effect, GO can adsorb on the friction surface during sliding to form a protective tribo-film related to its load-carrying capacity to fill and repair worn surfaces. However, the increasing intensity of Raman signals corresponding with concentration and the similar distribution of mapping are not convincing enough of the lubrication mechanism. The EDS lines crossing through the steel ball scars (Figs. 12(a)–12(d)) show the diversity of the chemical composition of the tribo-film. Lubrication mechanisms differ at lower and higher concentrations, depending on whether there is a chemical reaction. The results of the concentration with 1.00 and 5.00 mg/mL highlighted the C and O elements, illustrating that oxidation of carbon materials is involved in the formation of the friction protective film and protects the iron interface (Figs. 12(f) and 12(g)).

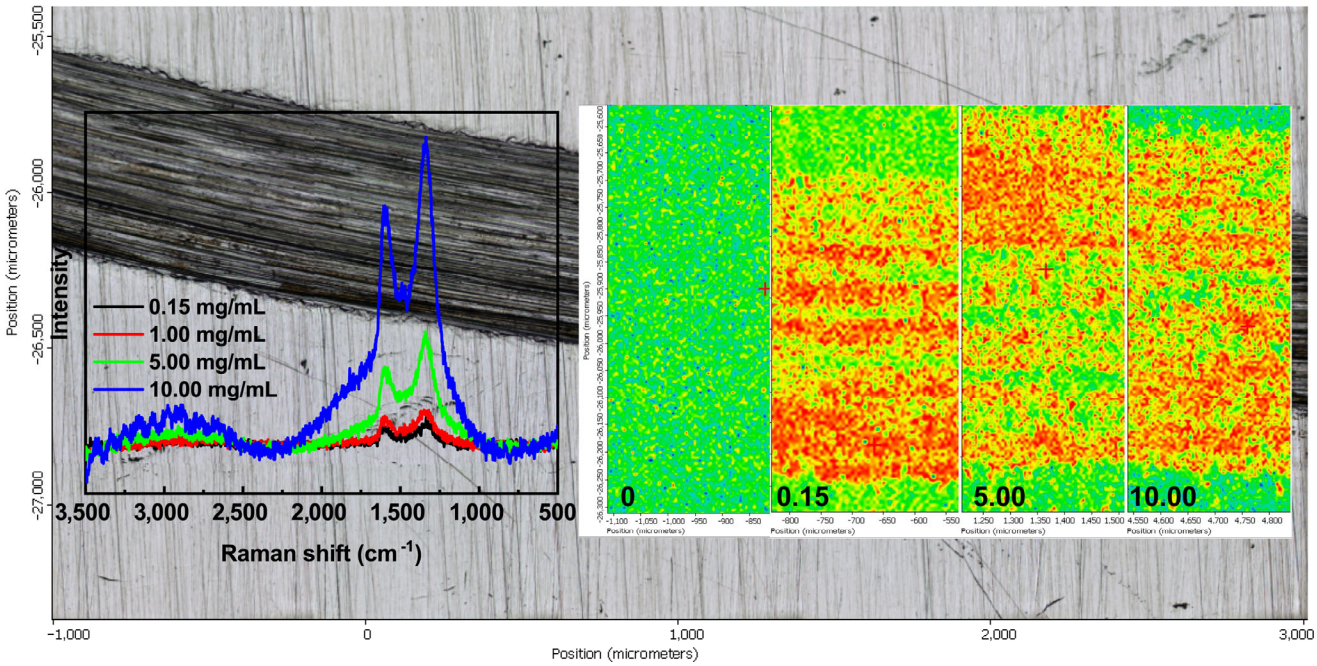

Fig. 11 2D Raman of the surface of wear scar after friction test. The background of figure is the optical photograph. The left figure shows the Raman spectra of dispersions with different GO concentrations (0–10.00 mg/mL). The right figure is the Raman mapping signals. The red area indicates the presence of GO.

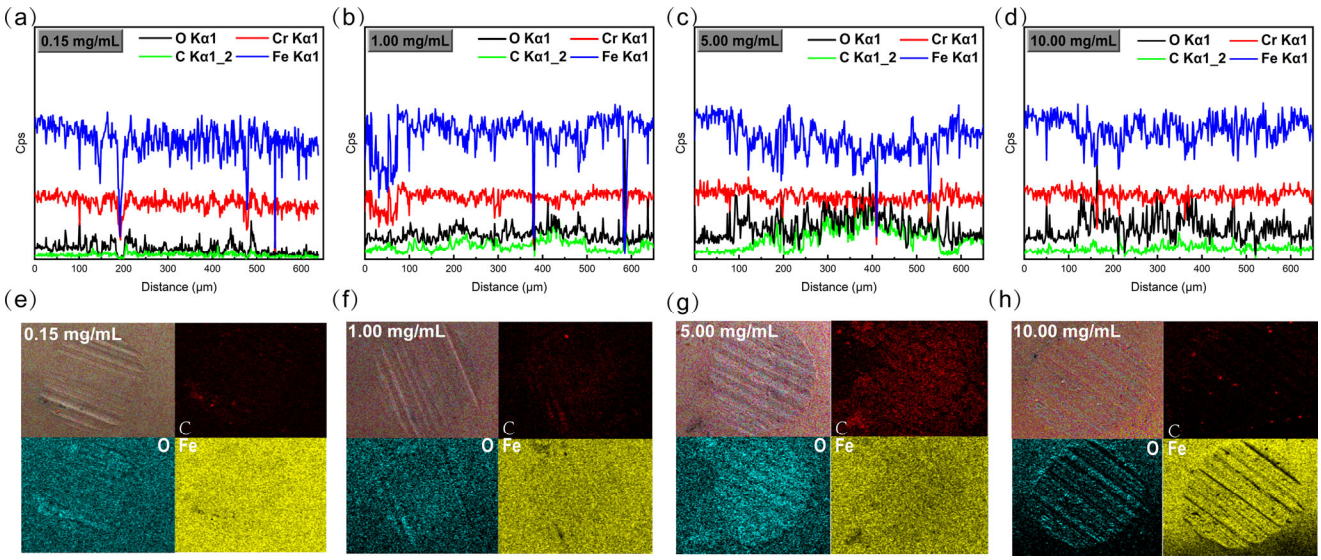

Fig. 12 EDS scan results of the scars on steel balls after friction test. (a–d) line and (e–h) mapping scan signals of the friction pairs of GO dispersions with different concentrations (0.15, 1.00, 5.00, 10.00 mg/mL).

The frictional film not only suffers the load of the steel ball but also prevents direct contact between the two mating metal surfaces. As a result, the anti-wear ability of the lubricant is improved and the coefficient of friction is significantly reduced and kept constant [61]. It can be seen from EDS-mapping that C is the most abundant element on the wear scar produced by 5.00 mg/mL, and Fe is the most abundant on the wear scar produced by 10 mg/mL, indicating that the formation of the liquid crystal phase and the formation of the friction film is not always working synergistically. When the aggregation effect causes agglomeration, it will lead to more serious wear of the friction pair.

During the fast shear sliding, the formation of the GOLC phase and tribo-film works simultaneously within different concentration ranges. At low concentration, GO is adsorbed to the interface and replenishes a tribo-film without the LC assembly and the aggregation effect. At high concentration, liquid crystal exists in advance and becomes more stick on the steel under shear conduct, actively participating in tribo-chemical reactions.

4 Conclusions

Graphene oxide is a promising water-based lubricant, however, dispersion stability has been a key challenge for applications. In this study, the formation of liquid crystals is proved to be an effective way to significantly improve the stability of GO water dispersion. The critical concentration of GO to form liquid crystal at 5.00 mg/mL was confirmed by SAXS and POM, and the rheological properties of GOLC were investigated by interfacial rheometer. It was found that GOLC could keep the low hydrophilic GO dispersion stable for several months via UV-Vis and aggregation degree observation. A low-viscosity and stable water-based lubricant is effectively realized, showing anti-wear and anti-wear properties vary in different concentration ranges. GO with a concentration as low as 0.15 mg/mL can decrease friction by 49.1% and wear by 41.7% compared to water before liquid crystal phase formation. When the liquid crystal phase is formed at the concentration of 5.00 mg/mL, it can decrease friction by 37.3% and wear by 25.2% compared to water, while it has longer stability than that at 0.15 mg/mL. The outstanding interfacial lubricating performance of the liquid crystal phase is due to the ordered structure that enhances the mechanical properties, bears the shear force in the normal direction, and protects the friction pair. However, the liquid crystal content has a limit on lubrication, since the aggregation effect brought by the high concentration of the additional amount under high-speed shearing leads to greater wear. Therefore, the development of GOLC lubricants needs comprehensively consideration (concentration, lateral size, etc.) of liquid crystal formation. It seems that GO with higher oxidation levels did not exhibit better anti-friction properties compared to GO with larger lateral dimensions. Certainly, further investigation is required deeply to reduced graphene oxide, which is potential applied as lubricant as well. In conclusion, the facile and readily available preparation, superior stability, and remarkable lubricating properties make the application of GO as a water-based lubricant of great significance.

Acknowledgements

We thank the Strategic Priority Research Program of the Chinese Academy of Sciences（No. XDB 0470000）, the International Partnership Program of Chinese Academy of Sciences project for Grand Challenges (No. 307GJHZ2022034GC) and the Science and Technology Development Fund of the Pudong New District (No. PKJ2020-N007) for the financial support, and the BL19U2 and BL01B beamlines of the National Facility for Protein Science in Shanghai (NFPS) at Shanghai Synchrotron Radiation Facility, for the support in the SAXS, WAXS, and synchrotron infrared micro-spectroscopy measurements (No. 2020-NFPS-PT-004482, h21pr0002).

Declaration of competing interest

The authors have no competing interests to declare that are relevant to the content of this article.

References

[1] Cognard J. Lubrication with liquid crystals. In *Tribology and the Liquid-Crystalline State.* American Chemical Society, 1990: 1–47.

[2] Gin D L, Pecinovsky C S, Bara J E, Kerr R L. Functional lyotropic liquid crystal materials. In *Liquid Crystalline Functional Assemblies and Their Supramolecular Structures*. Kato T (Ed). Springer, 2008:181–222.

[3] Tjipto-Margo B, Evans G T. The Onsager theory of the isotropic–nematic liquid crystal transition: Incorporation of the higher virial coefficients. *J Chem Phys* **93**(6): 4254–4265 (1990)

[4] Ohadi D, Corti D S, Uline M J. On using the BMCSL equation of state to renormalize the Onsager theory approach to modeling hard prolate spheroidal liquid crystal mixtures. *Entropy* **23**(7): 846 (2021)

[5] Sasikala S P, Lim J, Kim I H, Jung H J, Yun T, Han T H, Kim S O. Graphene oxide liquid crystals: A frontier 2D soft material for graphene-based functional materials. *Chem Soc Rev* **47**(16): 6013–6045 (2018)

[6] Kim F, Cote L J, Huang J X. Graphene oxide: Surface activity and two-dimensional assembly. *Adv Mater* **22**(17): 1954–1958 (2010)

[7] Kim J, Cote L J, Kim F, Yuan W, Shull K R, Huang J X. Graphene oxide sheets at interfaces. *J Am Chem Soc* **132**(23): 8180–8186 (2010)

[8] Paulista Neto A J, Fileti E E. Elucidating the amphiphilic character of graphene oxide. *Phys Chem Chem Phys* **20**(14): 9507–9515 (2018)

[9] Kim J, Cote L J, Huang J X. Two dimensional soft material: New faces of graphene oxide. *Acc Chem Res* **45**(8): 1356–1364 (2012)

[10] Behabtu N, Lomeda J R, Green M J, Higginbotham A L, Sinitskii A, Kosynkin D V, Tsentalovich D, Parra-Vasquez A N G, Schmidt J, Kesselman E, *et al*. Spontaneous high-concentration dispersions and liquid crystals of graphene. *Nature Nanotech* **5**(6): 406–411 (2010)

[11] Kim J E, Han T H, Lee S H, Kim J Y, Ahn C W, Yun J M, Kim S O. Graphene oxide liquid crystals. *Angew Chem* **123**(13): 3099–3103 (2011)

[12] Lee K E, Kim S O. Graphene oxide liquid crystals special issue, editorial. *Part Part Syst Charact* **34**(9): 1700261 (2017)

[13] Xu Z, Gao C. Aqueous liquid crystals of graphene oxide. *ACS Nano* **5**(4): 2908–2915 (2011)

[14] Narayan R, Kim J E, Kim J Y, Lee K E, Kim S O. Graphene oxide liquid crystals: Discovery, evolution and applications. *Adv Mater* **28**(16): 3045–3068 (2016)

[15] Al-Zangana S, Iliut M, Turner M, Vijayaraghavan A, Dierking I. Confinement effects on lyotropic nematic liquid crystal phases of graphene oxide dispersions. *2D Mater* **4**(4): 041004 (2017)

[16] Aboutalebi S H, Gudarzi M M, Zheng Q B, Kim J K. Spontaneous formation of liquid crystals in ultralarge graphene oxide dispersions. *Adv Funct Mater* **21**(15): 2978–2988 (2011)

[17] Oh J Y, Park J, Jeong Y C, Kim J H, Yang S J, Park C R. Secondary interactions of graphene oxide on liquid crystal formation and stability. *Part Part Syst Charact* **34**(9): 1600383 (2017)

[18] Berman D, Erdemir A, Sumant A V. Graphene: A new emerging lubricant. *Mater Today* **17**(1): 31–42 (2014)

[19] Rosenkranz A, Liu Y Q, Yang L, Chen L. 2D nano- materials beyond graphene: From synthesis to tribological studies. *Appl Nanosci* **10**(9): 3353–3388 (2020)

[20] Zhao J, Gao T, Li Y R, He Y Y, Shi Y J. Two-dimensional (2D) graphene nanosheets as advanced lubricant additives: A critical review and prospect. *Mater Today Commun* **29**: 102755 (2021)

[21] He A S, Huang S Q, Yun J H, Jiang Z Y, Stokes J, Jiao S H, Wang L Z, Huang H. The pH-dependent structural and tribological behaviour of aqueous graphene oxide suspensions. *Tribol Int* **116**: 460–469 (2017)

[22] Liu L C, Zhou M, Jin L, Li L C, Mo Y T, Su G S, Li X, Zhu H W, Tian Y. Recent advances in friction and lubrication of graphene and other 2D materials: Mechanisms and applications. *Friction* **7**(3): 199–216 (2019)

[23] Zhang G Q, Xu Y, Xiang X Z, Zheng G L, Zeng X Q, Li Z P, Ren T H, Zhang Y D. Tribological performances of highly dispersed graphene oxide derivatives in vegetable oil. *Tribol Int* **126**: 39–48 (2018)

[24] Chouhan A, Kumari S, Sarkar T K, Rawat S S, Khatri O P. Graphene-based aqueous lubricants: Dispersion stability to the enhancement of tribological properties. *ACS Appl Mater Interfaces* **12**(46): 51785–51796 (2020)

[25] Guo P F, Chen L, Wang J J, Geng Z R, Lu Z B, Zhang G G. Enhanced tribological performance of aminated nano-silica modified graphene oxide as water-based lubricant additive. *ACS Appl Nano Mater* **1**(11): 6444–6453 (2018)

[26] Draude A P, Dierking I. Lyotropic liquid crystals from colloidal suspensions of graphene oxide. *Crystals* **9**(9): 455 (2019)

[27] Jalili R, Aboutalebi S H, Esrafilzadeh D, Konstantinov K, Razal J M, Moulton S E, Wallace G G. Formation and processability of liquid crystalline dispersions of graphene oxide. *Mater Horiz* **1**(1): 87–91 (2014)

[28] Sanjari Shahrezaei M A, Taheri S M R, Aboutalebi S H. Correlation of interfacial dilational rheology and processing of 2D Materials liquid crystals: A case-study of graphene oxide liquid crystal phases. *Iran J Phys Res* **20**(3): 515–524 (2020)

[29] Park H, Lee K H, Kim Y B, Ambade S B, Noh S H, Eom W, Hwang J Y, Lee W J, Huang J, Han T H. Dynamic assembly of liquid crystalline graphene oxide gel fibers for ion transport. *Sci Adv* **4**(11): eaau2104 (2018)

[30] Chouhan A, Mungse H P, Khatri O P. Surface chemistry of graphene and graphene oxide: A versatile route for their dispersion and tribological applications. *Adv Colloid Interface Sci* **283**: 102215 (2020)

[31] Zhao L, Yang H M, Liu C, Xue S Q, Deng Z, Li J S, Zeng X Q. The correlation between molecular structure and tribological properties of graphene oxide with different oxidation degree. *Tribol Lett* **67**(3): 1–19 (2019)

[32] Golchin A, Wikner A, Emami N. An investigation into tribological behaviour of multi-walled carbon nanotube/graphene oxide reinforced UHMWPE in water lubricated contacts. *Tribol Int* **95**: 156–161 (2016)

[33] Lee D W, De Los Santos V L, Seo J W, Felix L L, Bustamante D A, Cole J M, Barnes C H W. The structure of graphite oxide: Investigation of its surface chemical groups. *J Phys Chem B* **114**(17): 5723–5728 (2010)

[34] Cuong T V, Pham V H, Tran Q T, Hahn S H, Chung J S, Shin E W, Kim E J. Photoluminescence and Raman studies of graphene thin films prepared by reduction of graphene oxide. *Mater Lett* **64**(3): 399–401 (2010)

[35] Sun L. Structure and synthesis of graphene oxide. *Chin J Chem Eng* **27**(10): 2251–2260 (2019)

[36] Cote L J, Kim J, Tung V C, Luo J Y, Kim F, Huang J X. Graphene oxide as surfactant sheets. *Pure Appl Chem* **83**(1): 95–110 (2010)

[37] Hu X B, Yu Y, Zhou J E, Song L X. Effect of graphite precursor on oxidation degree, hydrophilicity and microstructure of graphene oxide. *Nano* **9**(3): 1450037 (2014)

[38] Poulin P, Jalili R, Neri W, Nallet F, Divoux T, Colin A, Aboutalebi S H, Wallace G, Zakri C. Superflexibility of graphene oxide. *Proc Natl Acad Sci U S A* **113**(40): 11088–11093 (2016)

[39] Xu Y, Nguyen Q, Malekahmadi O, Hadi R, Jokar Z, Mardani A, Karimipour A, Ranjbarzadeh R, Li Z X, Bach Q V. Synthesis and characterization of additive graphene oxide nanoparticles dispersed in water: Experimental and theoretical viscosity prediction of non-Newtonian nanofluid. *Math Methods App Science*, https://doi.org/10.1002/mma.6381 (2020)

[40] Del Giudice F, Shen A Q. Shear rheology of graphene oxide dispersions. *Curr Opin Chem Eng* **16**: 23–30 (2017)

[41] Esfahani M R, Languri E M, Nunna M R. Effect of particle size and viscosity on thermal conductivity enhancement of graphene oxide nanofluid. *Int Commun Heat Mass Transf* **76**: 308–315 (2016)

[42] Kumar P, Maiti U N, Lee K E, Kim S O. Rheological properties of graphene oxide liquid crystal. *Carbon* **80**: 453–461 (2014)

[43] Abedin M J, Gamot T D, Martin S T, Ali M, Hassan K I, Mirshekarloo M S, Tabor R F, Green M J, Majumder M. Graphene oxide liquid crystal domains: Quantification and role in tailoring viscoelastic behavior. *ACS Nano* **13**(8): 8957–8969 (2019)

[44] Shim Y H, Ahn H, Lee S, Kim S O, Kim S Y. Universal alignment of graphene oxide in suspensions and fibers. *ACS Nano* **15**(8): 13453–13462 (2021)

[45] Vasu K S, Krishnaswamy R, Sampath S, Sood A K. Yield stress, thixotropy and shear banding in a dilute aqueous suspension of few layer graphene oxide platelets. *Soft Matter* **9**(25): 5874 (2013)

[46] Su Y J, Wei H, Gao R G, Yang Z, Zhang J, Zhong Z H, Zhang Y F. Exceptional negative thermal expansion and viscoelastic properties of graphene oxide paper. *Carbon* **50**(8): 2804–2809 (2012)

[47] Jyoti J, Babal A S, Sharma S, Dhakate S R, Singh B P. Significant improvement in static and dynamic mechanical properties of graphene oxide-carbon nanotube acrylonitrile butadiene styrene hybrid composites. *J Mater Sci* **53**(4): 2520–2536 (2018)

[48] Wang J A, Zhang K Y, Hao S A, Xia H S, Lavorgna M. Simultaneous reduction and surface functionalization of graphene oxide and the application for rubber composites. *J Appl Polym Sci* **136**(15): 47375 (2019)

[49] Fang S W, Chen T, Wang R, Xiong Y, Chen B, Duan M. Assembly of graphene oxide at the crude oil/water interface: A new approach to efficient demulsification. *Energy Fuels* **30**(4): 3355–3364 (2016)

[50] Yuan Q Q, Xue H, Lv J Y, Wang J J, Shi S W, Russell T P, Wang D. Size-dependent interfacial assembly of graphene oxide at water–oil interfaces. *J Phys Chem B* **124**(23): 4835–4842 (2020)

[51] Lu Y B, Franze K, Seifert G, Steinhäuser C, Kirchhoff F, Wolburg H, Guck J, Janmey P, Wei E Q, Käs J, *et al*. Viscoelastic properties of individual glial cells and neurons in the CNS. *Proc Natl Acad Sci U S A* **103**(47): 17759–17764 (2006)

[52] Nayar V T, Weiland J D, Nelson C S, Hodge A M. Elastic

and viscoelastic characterization of agar. *J Mech Behav Biomed Mater* **7**: 60–68 (2012)

[53] Naficy S, Jalili R, Aboutalebi S H, Gorkin R A, Konstantinov K, Innis P C, Spinks G M, Poulin P, Wallace G G. Graphene oxide dispersions: Tuning rheology to enable fabrication. *Mater Horiz* **1**(3): 326–331 (2014)

[54] Kamkar M, Erfanian E, Bazazi P, Ghaffarkhah A, Sharif F, Xie G H, Kannan A, Arjmand M, Hejazi S H, Russell T P, *et al*. Interfacial assembly of graphene oxide: From super elastic interfaces to liquid-in-liquid printing. *Adv Materials Inter* **9**(6): 2101659 (2022)

[55] Zhang L, Zhou J B, Yang H J, Wang X, Cai Z B, Zhu M H. Effect of modulation of interfacial properties on the tribological properties of viscoelastic epoxy resin damping coatings. *Polym Test* **100**: 107229 (2021)

[56] Lu X D, Zhao J, Mo J L, Wu Y K, Xu J W, Zhang Y F, Zhou Z R. Suppression of friction-induced stick-slip behavior and improvement of tribological characteristics of sliding systems by introducing damping materials. *Tribol Trans* **63**(2): 222–234 (2020)

[57] Richter M J, Schulz A, Subkowski T, Böker A. Adsorption and rheological behavior of an amphiphilic protein at oil/water interfaces. *J Colloid Interface Sci* **479**: 199–206 (2016)

[58] Singh S, Chen X C, Zhang C H, Tyagi R, Luo J B. Investigation on the lubrication potential of graphene oxide aqueous dispersion for self-mated stainless steel tribo-pair. *Vacuum* **166**: 307–315 (2019)

[59] Wychowaniec J K, Iliut M, Borek B, Muryn C, Mykhaylyk O O, Edmondson S, Vijayaraghavan A. Elastic flow instabilities and macroscopic textures in graphene oxide lyotropic liquid crystals. *NPJ 2D Mater Appl* **5**: 11 (2021)

[60] Babakhani P, Bridge J, Phenrat T, Doong R A, Whittle K R. Aggregation and sedimentation of shattered graphene oxide nanoparticles in dynamic environments: A solid-body rotational approach. *Environ Sci*: *Nano* **5**(8): 1859–1872 (2018)

[61] Song H J, Jia X H, Li N, Yang X F, Tang H A. Synthesis of α-Fe_2O_3 nanorod/graphene oxide composites and their tribological properties. *J Mater Chem* **22**(3): 895–902 (2012)

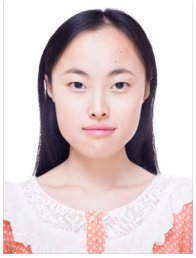

Yumei GUO. She received bachelor's degree from Chongqing University in 2019. Now she is studying for master's degree at Shanghai Advanced Research Institute, Chinese Academy of Sciences. Currently, she is working on the synthesis lyotropic liquid crystal and exploring the tribology and interfacial behaviors of lyotropic liquid crystal materials.

Xiangqiong ZENG. She received her Ph.D. degree in material science from Shanghai Jiao Tong University. She worked as staff scientist at Johnson & Johnson consumer group and then as assistant professor at University of Twente. Currently, she is a full professor at Shanghai Advanced Research Institute, Chinese Academy of Sciences, working on functional interfacial materials, including active control of friction, wear, and corrosion by surface and interface design and by additive and emulsion development.